Prediction of Contaminant Persistence in Aqueous Phase: A Quantum Chemical Approach

ARTICLE *in* ENVIRONMENTAL SCIENCE & TECHNOLOGY · FEBRUARY 2011

Impact Factor: 5.33 · DOI: 10.1021/es1028662 · Source: PubMed

4 AUTHORS, INCLUDING:

Jens Blotevogel
Colorado State University
15 PUBLICATIONS **50** CITATIONS
SEE PROFILE

Thomas Borch
Colorado State University
72 PUBLICATIONS **1,264** CITATIONS
SEE PROFILE

Environmental Science & Technology

ARTICLE

pubs.acs.org/est

Prediction of Contaminant Persistence in Aqueous Phase: A Quantum Chemical Approach

Jens Blotevogel,[†,‡] Arthur N. Mayeno,[§] Tom C. Sale,[‡] and Thomas Borch*[,†,∥]

[†]Department of Soil and Crop Sciences, Colorado State University, Fort Collins, Colorado 80523, United States

[‡]Department of Civil & Environmental Engineering, Colorado State University, Fort Collins, Colorado 80523, United States

[§]Department of Chemical & Biological Engineering, Colorado State University, Fort Collins, Colorado 80523, United States

[∥]Department of Chemistry, Colorado State University, Fort Collins, Colorado 80523, United States

Supporting Information

ABSTRACT: At contaminated field sites where active remediation measures are not feasible, monitored natural attenuation is sometimes the only alternative for surface water or groundwater decontamination. However, due to slow degradation rates of some contaminants under natural conditions, attenuation processes and their performance assessment can take several years to decades to complete. Here, we apply quantum chemical calculations to predict contaminant persistence in the aqueous phase. For the test compound hexamethylphosphoramide (HMPA), P−N bond hydrolysis is the only thermodynamically favorable reaction that may lead to its degradation under reducing conditions. Through calculation of aqueous Gibbs free energies of activation for all potential reaction mechanisms, it is predicted that HMPA hydrolyzes via an acid-catalyzed mechanism at pH < 8.2, and an uncatalyzed mechanism at pH 8.2-8.5. The estimated half-lives of thousands to hundreds of thousands of years over the groundwater-typical pH range of 6.0 to 8.5 indicate that HMPA will be persistent in the absence of suitable oxidants. At pH 0, where the hydrolysis reaction is rapid enough to enable measurement, the experimentally determined rate constant and half-life are in excellent agreement with the predicted values. Since the quantum chemical methodology described herein can be applied to virtually any contaminant or reaction of interest, it is especially valuable for the prediction of persistence when slow reaction rates impede experimental investigations and appropriate QSARs are unavailable.

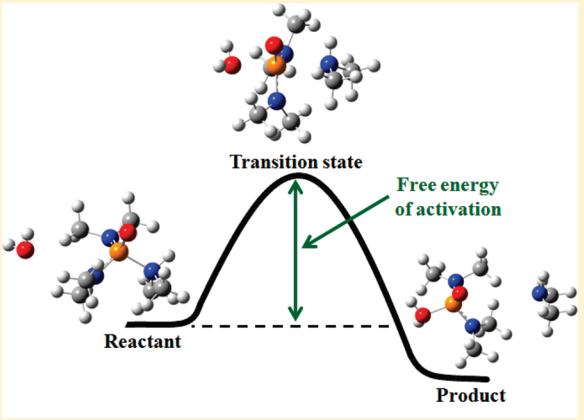

INTRODUCTION

Through inadvertent releases of chemicals, surface waters and groundwaters have become contaminated with a wide range of organic compounds, such as chlorinated solvents,[1] complex mixtures of hydrocarbons,[2] nitroaromatic compounds,[3] pesticides, personal care products, pharmaceuticals, steroid hormones,[4] and numerous other, often termed "new and emerging" contaminants.[5] Due to financial, technological, or other site-specific limitations, these contaminations cannot always be actively remediated, leaving natural attenuation (NA) as the only process that may lead to contaminant removal. Unfortunately, many of these compounds and their degradation products are poorly characterized with respect to their environmental fate or exhibit substantially different reactivity under different field conditions. Thus, to verify that monitored natural attenuation (MNA) is a viable (passive) remediation strategy at a specific site, contaminant mass loss, electron acceptor or donor consumption, and formation of degradation products must be assessed.[2] Depending on physicochemical and other properties that influence contaminant persistence as well as site-specific biogeochemical conditions,[6] NA processes may require long periods (years or decades) to achieve consequential contaminant losses.

An alternative to time-consuming experimental studies of the ever-increasing number of environmental contaminants, computational tools have been developed that can help assess their degradability and/or persistence. Currently, applied models for fate prediction are predominantly based on quantitative structure−activity relationships (QSARs).[7] However, QSAR-based predictions often fail when sufficient experimental data from structurally similar compounds are unavailable. To help overcome this limitation, we recently developed a quantum chemical approach that identifies the thermodynamic conditions necessary for redox-promoted degradation and predicts potential degradation pathways.[8] The overarching objective of this study is to estimate contaminant persistence based on quantum

Received: August 19, 2010
Accepted: January 28, 2011
Revised: January 18, 2011
Published: February 20, 2011

dx.doi.org/10.1021/es1028662 | Environ. Sci. Technol. 2011, 45, 2236–2242

chemical calculations of transformation kinetics, which can be used for any type of contaminant or reaction of interest, even for those lacking data on physicochemical properties or degradability. The underlying rationale for this prediction is the concept that the Gibbs free energy of activation, which can be determined from the difference in Gibbs free energy between transition state(s) and reactant(s), governs reaction rates according to transition state theory: the higher the free energy of activation, the lower the reaction rate (constant), and the longer the reaction half-life. Thus, once the major reaction pathway(s) have been determined and the reaction rate constant(s) (or half-lives) calculated, the persistence of a contaminant can be assessed.

As a test case for the prediction of contaminant persistence, hexamethylphosphoramide (HMPA, Figure 1), an extensively used solvent and groundwater contaminant,[9] is investigated here. Previous experimental studies have shown that HMPA-contaminated groundwater can be remediated through the application of permanganate, Fenton's reagent, or a combined UV/H_2O_2 process.[8,9] However, quantum chemical calculations indicated that HMPA oxidation is thermodynamically unfavorable below −30 mV at neutral pH. In the absence of suitable oxidants, hydrolysis of the P−N bond was predicted to be the only favorable reaction that may lead to its degradation ($\Delta_r G^0_{(aq)}$ = −37 kJ/mol).[8] In the same study, however, no hydrolysis of HMPA was experimentally observed over the course of six months at pH 7.

Transformation of a reactant to its product(s) may occur via more than just one transition state, i.e., a single product may arise via different reaction mechanisms. Consequently, all plausible reaction mechanisms should be investigated to maximize prediction accuracy. Mechanisms can be determined based on potential energy surface scans, expert knowledge, and/or literature studies. The reaction path(s) with the lowest free energy of activation govern(s) the total reaction rate. For P−N bond hydrolysis in tetracoordinate phosphorus compounds like HMPA, four general mechanisms have previously been reported to be theoretically possible (Figure 1):[10] (1) a stepwise associative mechanism (addition−elimination, $S_N2I@P$) with a pentacoordinate intermediate, (2) a stepwise dissociative mechanism (elimination-addition, $S_N1@P$) with a tricoordinate intermediate, (3) a concerted frontside mechanism ($S_N2@P$-f), and (4) a concerted backside mechanism ($S_N2@P$-b), with the latter two each having one pentacoordinate transition state in which water attacks the central phosphorus atom at the same time as one of the dimethylamine substituents is leaving. In addition, the reaction can be catalyzed by protons at low pH (e.g., A2@P mechanism) and by hydroxide ions at high pH.

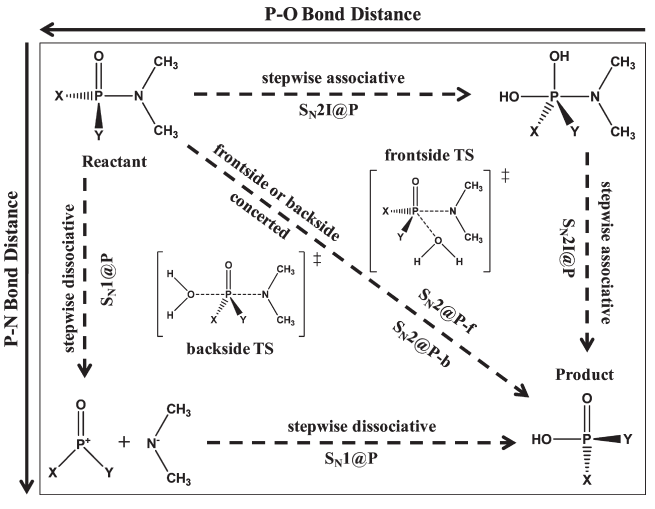

Figure 1. Conceptual potential energy surface and potential mechanisms of P−N bond hydrolysis, indicating changes in P−O and P−N bond distances during reaction. X and Y are arbitrary substituents (for HMPA, X = Y = $N(CH_3)_2$); chirality of the product is dependent on actual mechanism. TS = transition state.

Acid-catalyzed hydrolysis of phosphoric triamide (three P−N bonds), as well as many other tetracoordinate phosphorus amides, such as phosphorodiamidates (one P−O and two P−N bonds), phosphonamides (one P−C and two P−N bonds), and phosphinamides (one P−N and two P−C bonds), was suggested to proceed via an A2@P mechanism, i.e., initial protonation of the nitrogen with a subsequent concerted $S_N2@P$ reaction (Scheme 1).[10−14]

The activation of the P−N bond through protonation greatly increases hydrolysis rates as it makes the nitrogen-containing substituent a better leaving group, which is reflected by a first order dependence of the rate constant on proton activity.[15] Whereas acid-catalyzed hydrolysis can be the predominant mechanism for tetracoordinate phosphorus amides at near-neutral pH, the base-catalyzed mechanism was shown to contribute to the total rate of hydrolysis in phosphoramide only at pH values greater than 9,[14] and it was thus not investigated here. The mechanism for uncatalyzed P−N bond hydrolysis in phosphoramide compounds like HMPA, however, has not yet been elucidated due to the slow reaction rates at neutral pH,[13] which impede experimental investigations.

In this article, we investigate the mechanisms of P−N bond hydrolysis in HMPA, calculate Gibbs free energies of activation, and estimate reaction rate constants and half-lives as a function of pH, using density functional theory (DFT) and a cluster-continuum solvation model.[16] The specific objective of this study is to assess the persistence of aqueous HMPA in the absence of suitable oxidants over the groundwater-typical pH range of 6.0 to 8.5.

COMPUTATIONAL DETAILS

Quantum chemical calculations were conducted to investigate the mechanisms and kinetics of HMPA hydrolysis. All calculations were performed via Gaussian 03 using the B3LYP hybrid functional, without symmetry constraints, and default settings unless noted otherwise. Potential energy minima for reactants and intermediates were verified by frequency calculations (i.e., no imaginary frequencies). First-order saddle points (transition states) were verified by both frequency (i.e., exactly one imaginary frequency) and intrinsic reaction coordinate (IRC) calculations.

Scheme 1

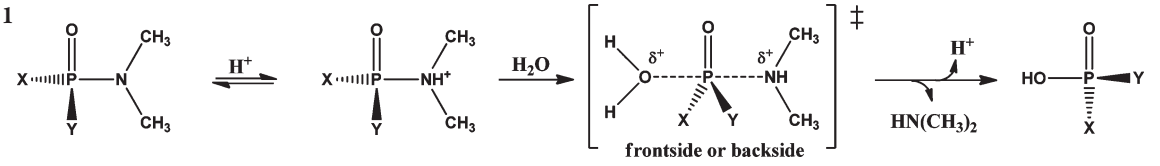

To account for solvation effects on reaction mechanisms and rates, a cluster-continuum solvation model[17] was applied. In the cluster-continuum approach, a (limited) number of explicit solvent molecules are placed around the reactant(s) and studied using an implicit continuum solvation model (for details, see the Supporting Information). Initially, the ideal number of explicit solvent molecules[17] was determined for each of the potential hydrolysis mechanisms. For this task, reactant, intermediate (INT), and transition state (TS) structures were optimized in the gas phase. Explicit water molecules were then sequentially added until the determined free energies stabilized. For the S_N2I@P, S_N1@P, and S_N2@P-f mechanisms, the 6-31+G(d) basis set was used on all elements. For the S_N2@P-b and A2@P mechanisms, however, the transition states could only be located when a second d-orbital was used for phosphorus; these transition states were initially optimized using the 6-31G(d) basis set on C, H, N, and O as well as the 6-31G(2d) basis set on P.

After determination of the ideal number of explicit water molecules, all respective lowest-energy ground and transition states including explicit solvation were optimized at the B3LYP/6-31+G(d) level of theory (6-31+G(2d) on P) with the integral equation formalism polarizable continuum model (IEFPCM).[18] Subsequently, single-point energy calculations were performed on the optimized geometries at the B3LYP/6-311++G(3df,3pd) level of theory in combination with IEFPCM.

Due to convergence problems[19,20] that occurred during one of our IEFPCM model calculations using Gaussian 03, the newer Gaussian 09 was used to optimize the ground state structure of the S_N2@P-b mechanism, which included six explicit water molecules. For this calculation, the default Gaussian 09 IEFPCM settings were replaced by Gaussian 03 default IEFPCM settings. A subsequent frequency analysis of the optimized structure in Gaussian 03 showed no imaginary frequencies.

The Gibbs free energies of reaction, $\Delta_r G_{(aq)}$, and the Gibbs free energies of activation, $\Delta^{\ddagger} G_{(aq)}$, in aqueous phase at 22 °C (same temperature as our experimental system) were calculated from the total free energies in solution and the thermal corrections to Gibbs free energy from a frequency analysis at 295.15 K. Pseudo-first-order rate constants (k_i, with i = 1, 2) were calculated via transition state theory[21]

$$k_i = \kappa \left(\frac{k_B T}{h}\right) \exp\left(\frac{-\Delta^{\ddagger} G_{(aq)}}{RT}\right)$$

where k_B is the Boltzmann constant, T is the temperature in Kelvin, h is Planck's constant, R is the universal gas constant, and κ is the transmission coefficient which accounts for quantum mechanical tunneling effects[22]

$$\kappa = 1 + \frac{1}{24}\left(\frac{1.44\nu_i}{T}\right)^2$$

where ν_i is the magnitude of the imaginary frequency in cm^{-1} corresponding to the reaction coordinate at the transition state. For uncatalyzed hydrolysis, the predicted rate constant k_1 is with respect to the activity of HMPA (i.e., $r = k_1\{HMPA\}$, where r is the hydrolysis rate), and for acid-catalyzed hydrolysis, the predicted rate constant k_2 is with respect to the activity of the protonated species HMPA-H^+ (i.e., $r = k_2\{HMPA\text{-}H^+\}$).

A total pseudo-first-order rate constant k_{hyd} for HMPA hydrolysis, where r_{tot} is the total reaction rate and the total HMPA activity $\{HMPA_{tot}\} = \{HMPA\} + \{HMPA\text{-}H^+\}$, is defined in the rate equation

$$r_{tot} = k_{hyd}\{HMPA_{tot}\} = k_1\{HMPA\} + k_2\{HMPA\text{-}H^+\}$$

The activity of the protonated species depends on its acidity constant K_a and the proton activity

$$\{HMPA\text{-}H^+\} = \frac{\{HMPA\}\{H^+\}}{K_a}$$

Substitution and rearrangement then yield the equation that was used to calculate k_{hyd} from the quantum chemically predicted k_1 and k_2

$$k_{hyd} = \left[\frac{k_1 K_a + k_2\{H^+\}}{K_a + \{H^+\}}\right]$$

Pseudo-first-order reaction half-lives $t_{1/2}$ were calculated via

$$t_{1/2} = \frac{\ln 2}{k_{hyd}}$$

EXPERIMENTAL SECTION

To experimentally determine k_{hyd}, the hydrolysis of HMPA over time was measured. Triplicates of DI water (100 mL) were adjusted to pH 0 with HCl (37%) in 250-mL Pyrex media glass bottles sealed with PTFE-faced silicone septa. The pH was measured with a UP-25 pH/mV/Ion Meter (Denver Instruments). HMPA (40 μL, 99% purity, MP Biomedicals) was added, and the reaction bottles were stored in the dark without agitation at 22 °C. Samples for analysis (15 μL) were diluted 1:100 with a NaOH solution of pH 12, resulting in a pH of 7, at which HMPA hydrolysis was shown to be negligible over a period of at least six months.[8] The samples were analyzed with an Agilent 1100 Series liquid chromatograph equipped with a 150 mm × 2.1 mm XTerra Phenyl column, 3.5 μm particle size (Waters), in combination with an Agilent G3250AA MSD TOF system (LC/MS-TOF). Separation was carried out isocratically with 0.01% formic acid/acetonitrile (98:2) as described previously.[8]

RESULTS

To predict the reaction rates and half-lives for HMPA hydrolysis over the groundwater-typical pH range of 6.0 to 8.5, the potential reaction mechanisms outlined in the Introduction were investigated computationally.

Associative Stepwise Mechanism. In the first transition state (TS1, $\Delta^{\ddagger} G_{(aq)}$ = 189 kJ/mol, Figure 2) of the S_N2I@P mechanism (Figure 1), the attacking nucleophile H_2O transfers a proton to the oxygen that is double-bonded to the central phosphorus atom, while the remaining hydroxyl group forms a new covalent bond with phosphorus. For the formed pentacoordinate intermediate (INT, $\Delta_r G_{(aq)}$ = 182 kJ/mol, Figure 2), a pseudorotation mechanism, as reported previously for some lower molecular weight phosphorus compounds,[23] could not be found, possibly due to steric hindrance imposed by the bulky dimethylamine substituents. Rather, direct proton transfer proceeds through a second TS (TS2, $\Delta^{\ddagger} G_{(aq)}$ = 212 kJ/mol, Figure 2), forming tetramethylphosphoric diamide as the product.

Dissociative Stepwise Mechanism. The heterolytic dissociation of the P−N bond (to form the ionic intermediate; Figure 1) is predicted to have a $\Delta_r G_{(aq)}$ of +215 kJ/mol in

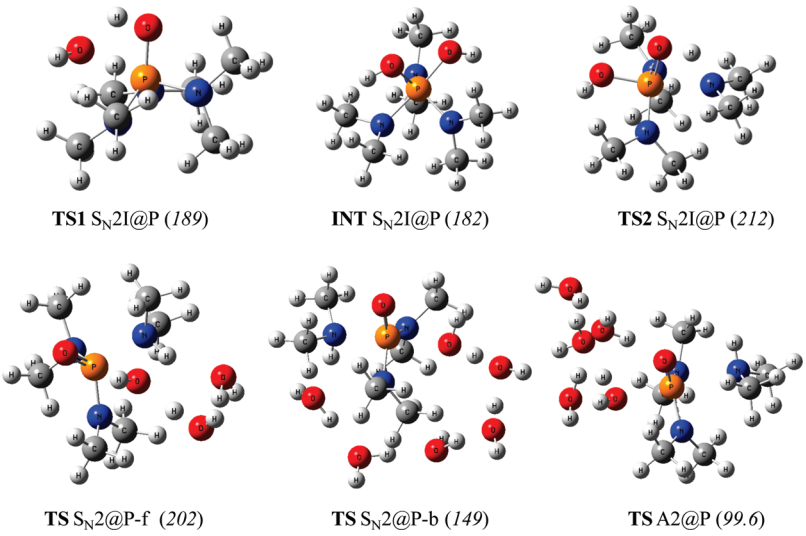

Figure 2. Optimized geometries of stationary points for HMPA hydrolysis in aqueous phase. Values in parentheses are Gibbs free energies of activation (for transition states) and reaction (for the intermediate) in aqueous phase at 22 °C (kJ/mol). Enlarged illustrations showing the directions of the respective imaginary frequencies are included in the Supporting Information.

aqueous phase. Considering that the free energy of the transition state connecting the reactant with the intermediate must be equal to or higher than that of the intermediate, implying that the free energy of activation is ≥215 kJ/mol and thus significantly greater than that of all the other mechanisms considered (cf. Figure 2), the S_N1@P mechanism was ruled out without further determination of the transition states.

Concerted Frontside Mechanism. In the S_N2@P-f transition state ($\Delta^{\ddagger}G_{(aq)}$ = 202 kJ/mol, Figure 2), the attacking water molecule transfers a proton to the nitrogen atom within the leaving dimethylamine. The P−N bond lengthens from 1.70 Å in the ground state to 1.93 Å in the transition state, while the resulting hydroxide ion approaches the phosphorus to subsequently form a covalent P−O bond. A concerted proton relay transfer mechanism, in which the proton on the nitrogen stems from a different water cluster molecule than the attacking nucleophile H_2O molecule, could not be located due to steric hindrance by the methyl substituents.

Concerted Backside Mechanism. In the S_N2@P-b mechanism (Figure 1, ν_i = 814 cm^{-1}), H_2O attacks the phosphorus on one side to form a P−OH bond, requiring proton transfer to remove the excess proton. On the opposite side of the phosphorus, the leaving dimethylamine substituent is a potent proton acceptor. To avoid unrealistic (destabilizing) charge separation in the transition state and enable proton transfer through the solvent water between the phosphorus-attacking water molecule and the leaving dimethylamine substituent, model systems containing at least five explicit water molecules were created and evaluated. Five was the minimum number of water molecules to allow the solvent cluster to span the HMPA molecule. In the lowest-energy conformation of the backside transition state (Figure 2: S_N2@P-b), which included six explicit water molecules, the P−N bond distance is 0.07 Å longer (i.e., a total distance of 2.00 Å) compared to the frontside attack. The free energy of activation in aqueous phase for the S_N2@P-b mechanism (149 kJ/mol) was determined to be 53 kJ/mol lower than for the frontside mechanism.

Acid-Catalyzed Concerted Backside Mechanism. For the hydrolysis of the protonated species, we inferred that the backside mechanism is the kinetically most favorable mechanism, based on the substantially lower activation barrier of the backside over the frontside S_N2@P mechanism for the uncatalyzed P−N bond hydrolysis, and the assumption that the steric effects are similar for both uncatalyzed and acid-catalyzed hydrolysis. Thus, only the backside A2@P mechanism was investigated to elucidate acid-catalyzed P−N bond hydrolysis.

In the ground state of the *N*-protonated HMPA species, the P−N bond distance is 0.14 Å longer than in the unprotonated species (i.e., 1.85 Å vs 1.71 Å). In the transition state (Figure 2: A2@P, ν_i = 173 cm^{-1}), which is stabilized by four additional explicit water molecules, the P−N bond distance is 0.47 Å longer than in the uncatalyzed S_N2@P-b mechanism (i.e., 2.47 Å). The free energy of activation in aqueous phase for acid-catalyzed P−N bond hydrolysis (99.6 kJ/mol) is 50 kJ/mol lower than for the uncatalyzed mechanism.

Prediction of Reaction Rate and Half-Life at 22 °C. P−N bond hydrolysis of the unprotonated HMPA molecule is independent of the pH, which is reflected by a straight line with a slope of zero when the pseudo-first-order rate constant k is plotted against the pH (Figure 3). For acid-catalyzed P−N bond hydrolysis, k depends on both the pH and the acidity constant K_a of HMPA, as described in the Computational Details section. Since an experimental pK_a (with pK_a = -logK_a) is unavailable, we estimated it to be −0.38 using SPARC.[24] The plot of log$k$ vs pH yields a straight line with a slope of −1, indicative of the first-order dependence of acid-catalyzed P−N bond hydrolysis on pH.[15] This A2@P mechanism dominates P−N bond hydrolysis at pH values <8.2. The uncatalyzed S_N2@P-b mechanism only predominates at pH > 8.2 and becomes a noticeable contributor to the total rate constant k_{hyd} only at pH values greater than ca. 7.

Moreover, Figure 3 indicates that the predicted half-life of P−N bond hydrolysis is 3500 years at pH 6, 33,000 years at pH 7, and 370,000 years at pH 8.5. An increase in proton activity substantially decreases half-lives to time periods of less than one year at pH < 2.5. At pH 0, the rate constant of HMPA hydrolysis is predicted to be 0.0159 h^{-1}, corresponding to a half-life of 43.5 h.

Experimental Validation at 22 °C. To validate the theoretical prediction, the hydrolysis rate and half-life of HMPA were

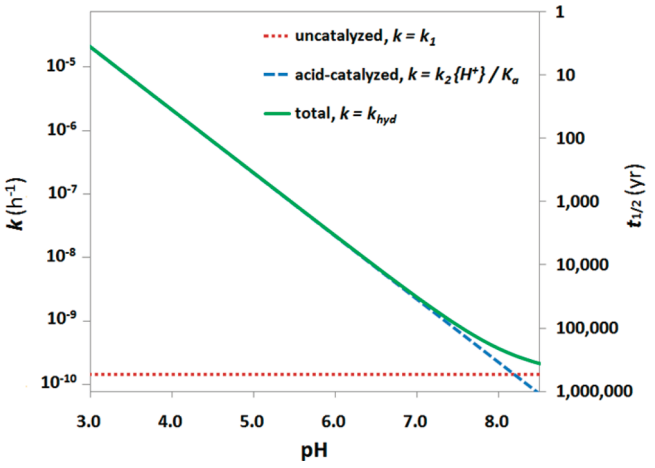

Figure 3. Predicted pseudo-first-order rate constants and half-lives at 22 °C for uncatalyzed, acid-catalyzed, and total P−N bond hydrolysis of HMPA.

measured at pH 0, at which the reaction was sufficiently rapid to enable experimental determination. The total pseudo-first-order rate constant k_{hyd} was found to be 0.00839 h^{-1} (see the Supporting Information), corresponding to a half-life of 82.6 h. Tetramethylphosphoric diamide was observed as the only product of HMPA degradation, confirming that P−N bond hydrolysis was the only reaction leading to its degradation. The mass-to-charge ratio (m/z) for the base peak $[M+H]^+$ of tetramethylphosphoric diamide with the molecular formula $PO_2N_2C_4H_{14}^+$ was measured to be 153.0787, with an error of −3.9 ppm with respect to the theoretical m/z of 153.0793.

In a parallel study at pH 7, which can be regarded as control for this experiment, neither hydrolysis nor any other reaction of HMPA were observed over a period of 6 months.[8]

DISCUSSION

Mechanisms, Rate Constants, and Half-Lives of HMPA Hydrolysis. To estimate reaction rate constants and half-lives, and ultimately to predict the persistence of HMPA in the absence of suitable oxidants, the potential P−N bond hydrolysis mechanisms and their free energies of activation in aqueous phase were computationally evaluated and compared.

The dissociative stepwise S_N1@P mechanism showed the highest free energy, indicating that it does not significantly contribute to the total rate of hydrolysis. This mechanism has previously been proposed for P−N bond hydrolysis in phosphoramidates with two P−O bonds, resulting in the formation of a metaphosphate intermediate (PO_3^-).[11,25] However, it has never been suggested to occur in tetracoordinate phosphorus amides with two or more P−N bonds. The associative stepwise S_N2I@P mechanism (assumed to be predominant in phosphinamides under base-catalyzed conditions[13]) and the frontside concerted S_N2@P-f mechanism are kinetically more favorable than the S_N1@P mechanism, but they are still negligible based on the calculated free energies of activation (>200 kJ/mol).

In previous experimental studies, the S_N2@P mechanism, or the corresponding acid-catalyzed A2@P mechanism, respectively, was proposed to be favored for tetracoordinate phosphorus amides that are structurally similar to HMPA, including phosphoramide.[10−14] Our calculations support this hypothesis for P−N bond hydrolysis of HMPA. However, it is specifically the backside concerted S_N2@P-b mechanism that is the main pathway for hydrolysis, as it is predicted to be 53 kJ/mol lower in free energy of activation compared to the frontside mechanism. This difference corresponds to a difference in reaction rate of almost 10 orders of magnitude, indicating that virtually no other mechanism than the concerted backside S_N2@P-b contributes to the uncatalyzed hydrolysis of the P−N bond, given that we have examined all realistic pathways and that the calculations are relatively accurate.

The acid-catalyzed A2@P mechanism, however, is the kinetically most favorable P−N bond hydrolysis mechanism for HMPA at pH values lower than 8.2. Despite the fact that only a minuscule amount of HMPA molecules is protonated at near-neutral pH (the pK_a was estimated to be −0.38), this mechanism is still favored due to a free energy of activation that is 47 kJ/mol lower than for the uncatalyzed mechanism (for 1 M HMPA or HMPA-H^+). The estimated crossing point for acid-catalyzed and uncatalyzed hydrolysis at pH 8.2 and 22 °C is comparable to the ones determined experimentally for phosphoramide of 8.30 at 30 °C and 8.46 at 15 °C.[14]

We note that there likely exists a base-catalyzed mechanism for HMPA hydrolysis as well. For phosphoramide, it was shown that base catalysis predominated at pH values of >9.7 at 15 °C and >9.0 at 30 °C.[14] However, as groundwater pH is typically in the range of 6.0-8.5, the base-catalyzed mechanism was not investigated here. Furthermore, for phosphoramidates (one P−N and two P−O bonds), it is known that P−N bond hydrolysis can be catalyzed biotically.[26] However, we are not aware of any reports on enzymatic P−N bond hydrolysis in HMPA. Thus, only abiotic mechanisms were considered in this study.

The experimental measurement of HMPA hydrolysis at pH 0 revealed that, for the A2@P mechanism, the computationally calculated reaction rate constant was overestimated, and thus the half-life was underestimated by a factor of 1.9. Consequently, HMPA is slightly more persistent than predicted by the methods used in this study. Three potential sources of error for this prediction are as follows: First, the B3LYP functional is known to systematically underestimate activation barriers,[27] resulting in an overestimation of the reaction rate (constant). Especially when relatively small basis sets are used, errors on the order of 20 kJ/mol have been reported.[27,28] Here, we have added a single-point energy calculation with a large basis set (6-311++G(3df,3pd)), which is a computationally efficient approach to increase the accuracy of the predicted energies.[29] Second, the cluster-continuum solvation model may introduce an error in solvation energies due to an arbitrary orientation of the water molecules in the incomplete first solvation shell.[30,31] This problem can be mitigated through the use of one or more full solvation shells,[30] which, however, is computationally very expensive when large molecules are investigated. When an incomplete first solvation shell is used, we generally found that more accurate solvation energies are obtained when the explicit water molecules are similarly oriented around the same functional group(s) in both ground and transition state complexes (for details, see the Supporting Information). Third, the pK_a for protonation of the nitrogen within the HMPA molecule of −0.38 had to be estimated using SPARC. This negative value appears to be within a reasonable range though, since comparable (i.e., slightly negative) pK_a values have been measured previously for dimethylamine substituents of structurally similar phosphinamides.[32] In a rigorous test estimating 4338 ionization constants, SPARC has

been shown to predict pK_a values with a root-mean-square deviation of 0.36 units for amino reaction centers.[24]

Comparisons of HMPA hydrolysis rate calculations at pH 0 using additional density functionals, basis sets, and solvation models are included in the Supporting Information. These calculations demonstrate that an appropriate level of theory was chosen for the predictive methodology presented here.

We note that reaction rates are very sensitive with respect to changes in activation barriers as well as changes in pK_a for pH-dependent reactions. A difference in free energy of activation of only 5.65 kJ/mol (at 22 °C), or a difference in pK_a of one unit for reactions with first-order dependence on proton activity, will change both reaction rate constant and half-life by 1 order of magnitude. A factor of 1.9, as observed in this prediction, corresponds to an error in free energy of activation of only 1.5 kJ/mol or an error in pK_a of 0.36. Thus, the predictive strategy applied here yields an estimation that is in excellent agreement with the experimental result, even though some of the introduced errors might have compensated each other.

Implications for the Environmental Fate of HMPA. In the absence of suitable oxidants, where P−N bond hydrolysis is the only thermodynamically favorable degradation reaction, HMPA is persistent over the groundwater-typical pH spectrum of 6.0-8.5. HMPA contains three P−N bonds that must be hydrolyzed to form the mineralization product *o*-phosphate as well as dimethylamine, which has been shown to be biodegradable under aerobic to methanogenic conditions.[33] However, predicted half-lives for the first hydrolysis step range from thousands to hundreds of thousands years at near-neutral pH. This hydrolysis is substantially slower than for phosphoramide, the product of HMPA oxidation by permanganate,[8] for which a half-life at pH 7 and 22 °C of 15 days can be derived from the kinetic parameters provided in ref 14. This rate is in agreement with experimental observations, which have shown that an increase in substituent size decreases P−N bond hydrolysis rates.[12,15] Therefore, natural attenuation (NA) processes are not effective for HMPA degradation under mildly to strongly reducing conditions at contaminated field sites. Only a substantial decrease in pH to values around 2−3 (or even lower at lower water temperatures) leads to appreciable reaction rates. However, acidification is not an option for in situ remediation due to adverse effects, such as ecosystem harm and heavy metal mobilization. Remediation by strong oxidants remains as viable strategy for HMPA-contaminated field sites.[8,9]

Implications for Contaminant Persistence Prediction. The results of this study illustrate that quantum chemical calculations can be successfully applied to predict contaminant persistence. Here, we have applied DFT calculations in combination with a cluster-continuum model to account for solvent effects, which has been shown to yield satisfactory solvation energies.[17,20,34] However, we re-emphasize that reaction rate (constant) and half-life predictions are very sensitive to errors in the calculation of Gibbs free energies of activation, such that the application of high levels of theory for the computation would be ideal, e.g., use of the computationally very expensive coupled cluster or configuration interaction methods.[28,35] Nevertheless, the predictive strategy presented here is a novel approach that can in general be applied to both redox- and nonredox-dependent degradation reactions without previous knowledge of a contaminant, especially when appropriate QSARs are unavailable or reaction rates are too slow to enable experimental measurement.

■ ASSOCIATED CONTENT

Supporting Information. Experimental determination of the HMPA hydrolysis rate constant at pH 0. Prediction using additional density functionals, basis sets, and solvation models. Vibration directions of the imaginary frequencies. Application of a cluster-continuum solvation model. This material is available free of charge via the Internet at http://pubs.acs.org.

■ AUTHOR INFORMATION

Corresponding Author

*Phone: (970)491-6235. Fax: (970)491-0564. E-mail: thomas.borch@colostate.edu. Corresponding author address: Department of Soil and Crop Sciences, 1170 Campus Delivery, Colorado State University, Fort Collins, CO 80523-1170, USA.

■ ACKNOWLEDGMENT

Primary funding for this work was provided by E.I. du Pont de Nemours and Company. Complementary support was provided by the University Consortium for Field-Focused Groundwater Contamination Research, a National Science Foundation (NSF) CAREER Award (EAR 0847683) to T. B., and NCSA through TeraGrid resources. We thank Dr. Anthony Rappé and Dr. Richard Casey for their invaluable help on this project.

■ REFERENCES

(1) Hunkeler, D.; Aravena, R.; Butler, B. J. Monitoring microbial dechlorination of tetrachloroethene (PCE) in groundwater using compound-specific stable carbon isotope ratios: Microcosm and field studies. *Environ. Sci. Technol.* **1999**, *33* (16), 2733–2738.

(2) Reineke, A. K.; Goen, T.; Preiss, A.; Hollender, J. Quinoline and derivatives at a tar oil contaminated site: Hydroxylated products as indicator for natural attenuation? *Environ. Sci. Technol.* **2007**, *41* (15), 5314–5322.

(3) Borch, T.; Inskeep, W. P.; Harwood, J. A.; Gerlach, R. Impact of ferrihydrite and anthraquinone-2,6-disulfonate on the reductive transformation of 2,4,6-trinitrotoluene by a gram-positive fermenting bacterium. *Environ. Sci. Technol.* **2005**, *39* (18), 7126–7133.

(4) Kolpin, D. W.; Furlong, E. T.; Meyer, M. T.; Thurman, E. M.; Zaugg, S. D.; Barber, L. B.; Buxton, H. T. Pharmaceuticals, hormones, and other organic wastewater contaminants in US streams, 1999−2000: A national reconnaissance. *Environ. Sci. Technol.* **2002**, *36* (6), 1202–1211.

(5) Richardson, S. D. Water analysis: Emerging contaminants and current issues. *Anal. Chem.* **2009**, *81* (12), 4645–4677.

(6) Borch, T.; Kretzschmar, R.; Kappler, A.; Van Cappellen, P.; Ginder-Vogel, M.; Voegelin, A.; Campbell, K. Biogeochemical redox processes and their impact on contaminant dynamics. *Environ. Sci. Technol.* **2010**, *44* (1), 15–23.

(7) Boethling, R. S.; Mackay, D. *Handbook of Property Estimation Methods for Chemicals: Environmental and Health Sciences*; CRC Press: Boca Raton, 2000.

(8) Blotevogel, J.; Borch, T.; Desyaterik, Y.; Mayeno, A. N.; Sale, T. C. Quantum chemical prediction of redox reactivity and degradation pathways for aqueous phase contaminants: An example with HMPA. *Environ. Sci. Technol.* **2010**, *44* (15), 5868–5874.

(9) Campos, D. Field demonstration of UV/H_2O_2 on the treatment of groundwater contaminated with HMPA. In *Chemical Oxidation: Technologies for the Nineties*; Eckenfelder, W. W., Bowers, A. R., Roth, J. A., Eds.; Technomic Publishing Company: Lancaster, 1997; Vol. 6, pp 19−26.

(10) Rahil, J.; Haake, P. Reactivity and mechanism of hydrolysis of phosphonamides. *J. Am. Chem. Soc.* **1981**, *103* (7), 1723–1734.

(11) Chanley, J. D.; Feageson, E. A study of hydrolysis of phosphoramides. II. Solvolysis of phosphoramidic acid and comparison with phosphate esters. *J. Am. Chem. Soc.* **1963**, *85* (8), 1181–1190.

(12) Garrison, A. W.; Boozer, C. E. The acid-catalyzed hydrolysis of a series of phosphoramidates. *J. Am. Chem. Soc.* **1968**, *90* (13), 3486–3494.

(13) Koizumi, T.; Haake, P. Acid-catalyzed and alkaline hydrolyses of phosphinamides. The lability of phosphorus-nitrogen bonds in acid and mechanisms of reaction. *J. Am. Chem. Soc.* **1973**, *95* (24), 8073–8079.

(14) Richter, S.; Töpelmann, W.; Lehmann, H. A. Hydrolysis of phosphoric acid amides. *Z. Anorg. Allg. Chem.* **1976**, *424* (2), 133–143.

(15) Haake, P.; Koizumi, T. Hydrolysis of phosphinamides and nature of P-N bond. *Tetrahedron Lett.* **1970**, *55*, 4845–4848.

(16) Pliego, J. R.; Riveros, J. M. The cluster-continuum model for the calculation of the solvation free energy of ionic species. *J. Phys. Chem. A* **2001**, *105* (30), 7241–7247.

(17) Pliego, J. R. Basic hydrolysis of formamide in aqueous solution: a reliable theoretical calculation of the activation free energy using the cluster-continuum model. *Chem. Phys.* **2004**, *306* (1−3), 273–280.

(18) Cances, E.; Mennucci, B.; Tomasi, J. A new integral equation formalism for the polarizable continuum model: Theoretical background and applications to isotropic and anisotropic dielectrics. *J. Chem. Phys.* **1997**, *107* (8), 3032–3041.

(19) Barone, V.; Cossi, M.; Tomasi, J. A new definition of cavities for the computation of solvation free energies by the polarizable continuum model. *J. Chem. Phys.* **1997**, *107* (8), 3210–3221.

(20) Stare, J.; Henson, N. J.; Eckert, J. Mechanistic aspects of propene epoxidation by hydrogen peroxide. Catalytic role of water molecules, external electric field, and zeolite framework of TS-1. *J. Chem. Inf. Model.* **2009**, *49* (4), 833–846.

(21) Eyring, H. The activated complex in chemical reactions. *J. Chem. Phys.* **1935**, *3* (2), 107–115.

(22) Raman, S.; Ashcraft, R. W.; Vial, M.; Klasky, M. L. Oxidation of hydroxylamine by nitrous and nitric acids. Model development from first principle SCRF calculations. *J. Phys. Chem. A* **2005**, *109*, 8526–8536.

(23) Chang, N. Y.; Lim, C. Factors governing the enhanced reactivity of five-membered cyclic phosphate esters. *J. Am. Chem. Soc.* **1998**, *120* (9), 2156–2167.

(24) Hilal, S. H.; Karickhoff, S. W.; Carreira, L. A. A rigorous test for SPARC′s chemical reactivity models: Estimation of more than 4300 ionization pK_as. *Quant. Struct.-Act. Relat.* **1995**, *14* (4), 348–355.

(25) Haake, P.; Allen, G. W. Studies on phosphorylation by phosphoroguanidinates. Mechanism of action of creatine: ATP transphosphorylase (creatine kinase). *Proc. Natl. Acad. Sci. U.S.A.* **1971**, *68* (11), 2691–2693.

(26) Abraham, T. W.; Kalman, T. I.; McIntee, E. J.; Wagner, C. R. Synthesis and biological activity of aromatic amino acid phosphoramidates of 5-fluoro-2′-deoxyuridine and 1-β-arabinofuranosylcytosine: Evidence of phosphoramidase activity. *J. Med. Chem.* **1996**, *39* (23), 4569–4575.

(27) Zhao, Y.; Truhlar, D. G. Hybrid meta density functional theory methods for thermochemistry, thermochemical kinetics, and noncovalent interactions: The MPW1B95 and MPWB1K models and comparative assessments for hydrogen bonding and van der Waals interactions. *J. Phys. Chem. A* **2004**, *108* (33), 6908–6918.

(28) Zhang, Q.; Bell, R.; Truong, T. N. *Ab initio* and density functional theory studies of proton transfer reactions in multiple hydrogen bond systems. *J. Phys. Chem.* **1995**, *99* (2), 592–599.

(29) Paul, K. W.; Kubicki, J. D.; Sparks, D. L. Quantum chemical calculations of sulfate adsorption at the Al- and Fe-(hydr)oxide-H_2O interface - Estimation of Gibbs free energies. *Environ. Sci. Technol.* **2006**, *40* (24), 7717–7724.

(30) Bryantsev, V. S.; Diallo, M. S.; Goddard, W. A. Computational study of copper(II) complexation and hydrolysis in aqueous solutions using mixed cluster/continuum models. *J. Phys. Chem. A* **2009**, *113* (34), 9559–9567.

(31) Kamerlin, S. C. L.; Haranczyk, M.; Warshel, A. Are mixed explicit/implicit solvation models reliable for studying phosphate hydrolysis? A comparative study of continuum, explicit and mixed solvation models. *ChemPhysChem* **2009**, *10* (7), 1125–1134.

(32) Haake, P.; Koizumi, T. Basicity of phosphinamides and site of protonation. *Tetrahedron Lett.* **1970**, *55*, 4849–4850.

(33) van Agteren, M. H.; Keuning, S.; Janssen, D. B. *Handbook on Biodegradation and Biological Treatment of Hazardous Organic Compounds*; Kluwer Academic Publishers: Norwell, 1998.

(34) Nguyen, M. T.; Raspoet, G.; Vanquickenborne, L. G. Necessity to consider a three-water chain in modelling the hydration of ketene imines and carbodiimides. *J. Chem. Soc., Perkin Trans. 2* **1999**, No. 4, 813–820.

(35) Niu, S. Q.; Hall, M. B. Comparison of Hartree-Fock, density functional, Møller-Plesset perturbation, coupled cluster, and configuration interaction methods for the migratory insertion of nitric oxide into a cobalt-carbon bond. *J. Phys. Chem. A* **1997**, *101* (7), 1360–1365.